HHS Public Access

Author manuscript

Nat Cell Biol. Author manuscript; available in PMC 2018 September 12.

Published in final edited form as:

Nat Cell Biol. 2018 April ; 20(4): 413–421. doi:10.1038/s41556-018-0054-y.

Diminished apoptotic priming and ATM signalling confer a survival advantage onto aged haematopoietic stem cells in response to DNA damage

Paula Gutierrez-Martinez[*,1], **Leah Hogdal**[*,2], **Manavi Nagai**[1], **Miriama Kruta**[1], **Rumani Singh**[3], **Kristopher Sarosiek**[3], **Andre Nussenzweig**[4], **Isabel Beerman**[5], **Anthony Letai**[2,#], and **Derrick J. Rossi**

[1]Department of Stem Cell and Regenerative Biology, Harvard University, Cambridge, MA, USA. Program in Cellular and Molecular Medicine, Division of Hematology/Oncology, Boston Children's Hospital, Boston, MA, USA

[2]Dana-Farber Cancer Institute, Harvard Medical School, Boston, MA 02215, USA

[3]John B. Little Center for Radiation Sciences, Department of Environmental Health, Harvard T. H. Chan School of Public Health, Boston, MA 02115, USA

[4]Laboratory of Genome Integrity, National Cancer Institute, NIH, Bethesda, MD 20892, USA

[5]Translational Gerontology Branch, National Institute on Aging, NIH, Baltimore, MD

[6]Department of Stem Cell and Regenerative Biology, Harvard University, Cambridge, MA, USA. Program in Cellular and Molecular Medicine, Division of Hematology/Oncology, Boston Children's Hospital, Boston, MA, USA. Department of Pediatrics, Harvard Medical School, Boston, MA, USA Harvard Stem Cell Institute, Cambridge, MA, USA

Summary

Ageing of haematopoietic stem cells (HSC) contributes to deficits in the aged haematopoietic system. HSC decline is driven in part by DNA damage accumulation, yet how aging impacts the acute DNA damage response (DDR) of HSCs is poorly understood. We show that old HSCs exhibit diminished ATM activity and attenuated DDR leading to elevated clonal survival in response to a range of genotoxins that was underwritten by diminished apoptotic priming. Distinct HSC subsets exhibited ageing-dependent and subtype-dependent differences in apoptotic priming and survival in response to DNA damage. The defective DDR of old HSCs was non-cell autonomous as ATM signalling, and clonal survival in response to DNA damage could be restored

[#]co-corresponding authors, Anthony_Letai@dfci.harvard.edu, Derrick.Rossi@childrens.harvard.edu.
[*]These authors contributed equally to this study.

Author Contributions

P.G-M. designed, performed and analysed most experiments and wrote the manuscript, L.H. designed and performed BH3 profiling experiments, M.N. provided technical help, M.K. performed immunostainings, I.B. performed comet assays, transplantation of CD150 HSC subsets and provided critical guidance, R.S. and K.S. provided $Bax^{-/-}$ and $Bak^{-/-}$ mice, A.N. provided $ATM^{-/-}$ mice and ATM guidance, and A.L. and D.J.R. designed experiments and wrote the manuscript.

The authors declare that they have no competing financial interests.

to levels observed in young HSCs post-transplantation into young recipients. These data suggest that defective DDR and diminished apoptotic priming provide a selective advantage to old HSCs that may contribute to mutation accrual and disease predisposition.

Introduction

Stem cells mediate tissue homeostasis and regeneration, and ageing-associated decline in stem cell compartments contributes to pathophysiology in multiples tissues and organ systems[1,2]. Diminished haematopoietic stem cell (HSC) potential is a driver of ageing in the haematopoietic system[2,3,4]. Numerous mechanisms underlie HSC ageing including accumulation of DNA damage[5–8], alterations in transcriptional program[9,10], epigenetic remodeling[11,12], cell polarity changes[13], altered lineage output[14] and decreased regenerative potential[9,15–17]. Adult HSCs are largely quiescent which had been proposed to be a cytoprotective mechanism for preserving genome integrity and long-term function. However, it was recently shown that old HSCs have elevated levels of DNA damage at steady-state that are, at least in part, attributable to prolonged periods of dormancy[4]. Upon cell cycle entry, HSCs upregulate DNA damage response and repair pathways and repair accrued strand breaks[4].

Results

Aged HSCs show increased survival upon DNA damage induction in vitro and in vivo

As many cancers are treated with genotoxic agents[18], we investigated how HSCs respond to diverse types of DNA damage and whether this response is differentially regulated during ageing. To address this, single HSCs from young and old mice were sorted via the immunophenotype Lin-ckit+Sca1+Flk2-CD34-/lo Extendad data 2a), which are CD48− regardless of age (Supplemetary Figure 1 a, b), and exposed to different types of DNA damaging agents. These included N-ethyl-N-nitrosourea (ENU) and ethyl methanesulfonate (EMS) that induce point mutations, doxorubicin (Doxo) and gamma irradiation (IR) that produce double strand breaks (DSBs), and hydroxyurea (HU) that induces replicative stress (Fig. 1a). In the absence of challenge, young and old HSCs produced similar numbers of colonies when cultured in minimal media (yHSC: 64.7% +/− 14.3 and oHSC: 62.9% +/− 12.4) (Fig. 1b). Strikingly, oHSCs were invariably less sensitive to all genotoxic agents, exhibiting 2- to 6-fold elevated clonal survival than yHSCs depending upon the type of DNA damage induced (Fig. 1b, c). The elevated clonal survival of oHSCs could not be attributed to differences in cell cycle as both young and old HSCs showed similar cell cycle profiles when freshly isolated and after 18 hours of culture (Supplementary Figure 2b), as well as similar proliferation rates over the first 3 days of culture (Supplementary Figure 2c). Colony size 10-days post-plating was diminished after DNA damage induction irrespective of age indicating that the total proliferative output of surviving clones was ageing-independent (Supplementary Figure 2d, e). The differential survival response to DNA damage induction was specific to oHSCs as single myeloid progenitors (MPs, Lin-ckit+Sca1−) exposed to EMS, ENU and IR, and multipotent progenitors (MPP1s, Lin-ckit+Sca1-CD34+Flk2− and MPP2s, Lin-ckit+Sca1-CD34+Flk2+) exposed to IR gave rise to colonies at similar frequencies (Fig. 1d-f) and sizes (Supplementary Figure 2f, g) regardless of age.

To further investigate the functional impact of DNA damage induction on HSCs, we isolated young and old HSCs, exposed them to either ENU or IR, and then competitively transplanted them into lethally irradiated congenic recipients. As previously reported[9,15,17], old HSCs showed significantly reduced total regenerative potential (Fig. 2a-b). However, whereas young HSCs exposed to either ENU or IR showed significantly reduced long-term reconstitution in comparison to young untreated HSCs, old HSCs exposed to either ENU or IR maintained long-term reconstitution potential comparable to untreated old HSCs (Fig. 2a, b). Old HSCs showed myeloid biased reconstitution as expected, and the lineage potentials of both young and old HSCs were unaltered by DNA damage induction (Fig. 2c, d).

Aged HSCs display elevated survival in response to DNA damage induction

The differential functional response of young and old HSCs observed *in vitro* (Fig. 1b, c) and *in vivo* (Fig. 2a-b) prompted us to explore clonal survival and growth dynamics in response to DNA damage induction. HSCs from young and old mice were clone sorted and were either untreated or exposed to IR, followed by culturing and analysis of viability and cell division daily for 8 days (n=288 clones/condition) (Supplementary Figure 2). As we had previously observed (Fig 1b), young HSC clones exposed to IR gave rise to significantly fewer viable colonies compared to untreated controls, whereas irradiated old HSCs showed no differences in survival compared to untreated old HSCs at any time point (Fig. 2e-g, Supplementary Figure 3). Strikingly, the greatest loss of viability of young clones occurred within the first 24 hours post-irradiation, prior to the first cell division (Fig. 2 e-g, Supplementary Figure 1c)[4], suggesting an intrinsic difference in the ability of young and old HSCs to respond to DNA damage. Consistent with clonal survival and transplantation data, old HSCs exhibited a diminished frequency of apoptotic (AnnexinV+/PI+) cells compared to young HSCs 8-hours post-irradiation but not at steady-state (Fig. 2h, i). This differential apoptotic response was specific to old HSCs as young and old MPs exposed to irradiation showed similar frequencies of apoptotic cells albeit at higher levels than observed for HSCs (Fig. 2h, i).

Aged HSCs exhibit diminished apoptotic priming

Apoptosis is regulated through a balance between pro- and anti-apoptotic members of the Bcl-2 family of proteins that control mitochondrial outer membrane permeabilization (MOMP) upstream of cytochrome-c release and caspase activation[19,20,21]. This family consists of pro-apoptotic BH3-only proteins, pro-apoptotic effector proteins and anti-apoptotic proteins, which interact to control MOMP. The BH3-only proteins are divided into two groups based on function - the “activators” (BIM and BID) and “sensitizers” (such as BAD, HRK and NOXA)[22]. The activators bind to and inhibit the anti-apoptotics, and also directly interact with and activate the effector proteins (BAX and BAK) causing the proteins to promote MOMP[23]. Anti-apoptotic proteins (such as BCL-2, BCL-XL and MCL-1) inhibit apoptosis by binding to BH3-only activators and effector proteins sequestering them from promoting apoptosis[24]. The BH3-only sensitizer proteins promote apoptosis by binding to the anti-apoptotic proteins, allowing for the release of the activator and effector proteins to initiate MOMP (Fig. 3a)[22,25,26]. Due to the complex interplay of the numerous proteins involved, combined with their many posttranslational modifications that can alter BCL-2 family protein function[27], BH3 profiling was developed as a method to evaluate the ability

of a cell to undergo apoptosis via the mitochondrial pathway[28–30]. This technique involves exposing mitochondria of permeabilized cells to peptides derived from the BH3 domains of BH3-only proteins, and quantifying MOMP, providing a measure of the readiness of cells to undergo apoptosis (subsequently referred to as apoptotic priming). We previously found that apoptotic priming predicts clinical response of cancers to cytotoxic chemotherapies[29,31] and governs healthy tissue sensitivity to ionizing radiation[32]. To determine if differences in apoptotic priming underlie the differential apoptotic response of young and old HSCs to DNA damage induction, we performed BH3 profiling on HSCs and downstream multi-potent and oligo-potent progenitors directly from the marrow of young and old mice (Supplementary Figure 4a). Young HSCs exposed to BIM peptide showed a trend towards diminished apoptotic priming in comparison to all downstream progenitors that reached statistical significance in comparison to CMP, GMP, MEPs and CLPs (Fig. 3b). This pattern was exacerbated in the bone marrow of old mice with HSCs showing significantly diminished priming in comparison to all downstream progenitors (Fig. 3b). Comparison of young versus old stem and progenitors revealed that HSCs, MPP1s, MPP2s, and oligopotent CMPs all showed significantly diminished priming in old mice, with HSCs showing the greatest differential (Fig. 3b). This pattern was largely mirrored upon exposure to BID peptide with old HSCs and multi-potent progenitors significantly less primed than their young counterparts (Fig. 3c). Experiments with HSCs from *Bax-/-* and *Bak-/-* mice showed that HSCs can undergo apoptosis via BAX and/or BAK as genetic deletion of either apoptosis effector diminished responses to their preferential activators, BIM and BID, respectively[33], but did not completely eliminate responses (Supplementary Figure 4b, c). Consistent with this, clonal survival upon irradiation was comparable in HSCs purified from $Bax^{-/-}$ or $Bak^{-/-}$ mice indicating functional redundancy of BAX and BAK in HSCs (Supplementary Figure 4d).

To assess the contribution of other BCL-2 family members to apoptotic priming in young and old HSCs, we interrogated the dependency of HSCs on the anti-apoptotic proteins BCL-2, BCL-XL and MCL-1 using BH3 peptides of the pro-apoptotic sensitizers BAD, HRK and NOXA which bind to BCL-2/BCL-XL, BCL-XL and MCL-1 respectively (Fig 3a). As we had observed with BIM and BID, old HSCs showed a significantly diminished response to BAD (Fig. 3d). Interestingly, murine HSCs exposed to NOXA peptides did not undergo MOMP irrespective of age indicating that dependency on anti-apoptotic function of MCL-1 may be less critical in steady-state HSCs than in other contexts[34–36]. In contrast, MPs were responsive to BAD, HRK and NOXA irrespective of age (Supplementary Figure 4e). Taken together, these data demonstrate that apoptotic response in steady-state HSCs is BIM-BAX- and BID-BAK-dependent. Furthermore, these pathways along with BAD-BCL2 are attenuated in old HSCs.

The primitive HSC compartment is heterogeneous[37–40]. HSC subsets bearing distinct lineage potentials can be discriminated based on differential expression of CD150 ($CD150^{hi}$, $CD150^{lo}$, $CD150^{neg}$)[14,41]. As expected, the frequency of myeloid-biased HSCs ($CD150^{hi}$) predominated the HSC compartment at the expense of lymphoid biased $CD150^{neg}$ HSCs in the bone marrow of old mice, as previously shown[3,14,41] (Fig. 4a, Supplementary Figure 4f). We therefore explored if the diminished apoptotic priming observed in old HSCs (Fig. 3b, c) could be attributable to these HSC subsets. Myeloid-biased $CD150^{hi}$ HSCs were

significantly less primed in response to BIM (old) and BID (young and old) than lymphoid-biased CD150^{neg} HSCs, while lineage balanced CD150^{lo} HSCs generally exhibited intermediate responses regardless of age (Supplementary Figure 4g). Comparison between young and old HSC CD150 subsets showed that apoptotic priming was significantly diminished with ageing in response to BIM and BID in all cases with the exception of CD150^{neg} in response to BIM (Fig. 4 b, c). Clonal survival in response to IR, and ENU revealed that lymphoid-biased CD150^{neg} HSCs were more sensitive to DNA damage induction showing reduced survival in comparison to myeloid-biased CD150^{hi} HSCs regardless of age (Fig. 4d). By contrast, exposure to doxorubicin resulted in significant differences in clonal HSC subset survival (Fig. 4d). In all cases the young HSC subsets were significantly more sensitive to doxorubicin treatment than their old counterparts, and myeloid-biased CD150^{hi} HSCs were the least sensitive regardless of age (Fig. 4d). Competitive transplantation of the HSC subsets from young and old mice showed that irradiation did not significantly alter the reconstitution potential of these HSC subsets regardless of age with the exception of lymphoid-biased CD150^{neg} HSCs purified from young bone marrow (Fig. 4e-g). Taken together, these data suggest that the differential response to DNA damage induction displayed by the old HSC compartment (Fig. 1–2) is in part underwritten by differences in apoptotic priming that are both ageing-dependent and HSC subtype-dependent.

Transplantation into a young host resets the DNA damage response of aged HSCs

Factors contributing to the decline of HSCs during ageing have largely been linked to cell autonomous mechanisms[5,6,9,11–17,42]. To address whether the ageing-dependent differences in the DNA damage response of HSCs (Figs. 1–3) are cell intrinsic, we transplanted young or old bone marrow cells into young recipients (Supplementary Figure 5 a, b) and then assayed apoptotic priming 21 to 23 weeks post-transplantation in comparison to untransplanted controls. In contrast to the steady-state in which old HSCs exhibited diminished apoptotic priming, the priming of old donor-derived HSCs post-transplantation into young recipients in response to BIM, BID and BAD was restored to levels comparable to those observed in young HSCs at steady state or post-transplantation (Fig. 5a). Apoptotic priming of myeloid progenitors examined post-transplantation was comparable to steady-state and unaltered regardless of donor age (Supplementary Figure 5c). To test if the normalization of apoptotic priming of old HSCs post-transplantation was concomitant with restoration of DDR, we assessed the ability of donor-derived HSC clones to form colonies upon irradiation. In contrast to the differences observed between young and old HSCs examined at steady-state (Fig. 1b), young and old donor-derived HSCs isolated post-transplantation into young recipients showed similar clonal survival in response to irradiation (Fig. 5b-d). We next asked whether exposure to an old microenvironment would reciprocally lower the apoptotic priming of young HSCs. Towards this, we transplanted young bone marrow cells into 17-month-old lethally irradiated recipients (Supplementary Figure 5d, e) and then assayed apoptotic priming 21 to 23 weeks post-transplantation. Surprisingly, donor-derived young HSCs showed higher levels of apoptotic priming than freshly isolated young HSCs (Fig. 5e). Interestingly, residual host HSCs of the old recipient also showed significantly higher apoptotic priming than untransplanted controls (Fig. 5e). Cumulatively, these results demonstrate that the diminished apoptotic priming of old HSCs

can be elevated upon transplantation into a young host to levels associated with young HSCs concomitant with a normalization of clonal survival upon exposure to DNA damage, and further suggest that the marrow microenvironment of old mice is altered post-irradiation leading to markedly elevated apoptotic priming of both donor-derived and host HSCs. At this stage, however, influences on apoptotic priming by the irradiation or transplantation procedure cannot be ruled out.

Aged HSCs have diminished ATM activity and DNA damage response (DDR)

The differential survival of young and old HSCs upon DNA damage induction (Figs 1–2) combined with the attenuated apoptotic priming (Fig. 3) prompted us to ask whether DNA damage signalling might be altered in old HSCs. We first analysed the expression of selected DNA damage response and sensor genes in young and old HSCs; of the 16 genes analysed, 5 (*Trp53, Atm, Chk1, Mre11 and Mdc1*) were age-regulated (Supplementary Figure 6a, b)[43]. Of these, *Trp53* was strongly upregulated in old HSCs, whereas all others were downregulated. Of the ageing-downregulated genes, *Atm*, *Mre11* and *Mdc1* encode proteins that coordinate DNA damage response with ATM being the master kinase responsible for signalling DSBs throughout the cell cycle, and MRE11 and MDC1 involved in stabilizing ATM signalling[44–46]. *Atm*-deficient HSCs exhibit profound deficiencies in reconstitution potential resulting from accumulation of reactive oxygen species (ROS)[47]. Furthermore, ATM phosphorylation of BID has been shown to be critical for HSC survival in response to irradiation[48]. This led us to test the competency of ATM signalling in response to DNA damage induction in young and old HSCs. Towards this, young and old HSCs that were either untreated or exposed to 2Gy irradiation were immuno-stained for γH2AX whose phosphorylation is ATM-dependent[49]. Consistent with previous reports in mice[5,50] and humans[8], old HSCs showed significantly greater numbers of γH2AX foci in the untreated samples (Fig. 6a, b). Strikingly, whereas young HSCs showed elevated γH2AX foci post-irradiation, old HSCs showed no change (Fig. 6a, b) even though DSBs were comparably induced by irradiation of both young and old HSC as shown by quantitation of 53BP1 irradiation induced foci[51] (Fig. 6 a, c) and comet assays (Supplementary Figure 6c, Fig 6f). The deficit in ATM signalling in old HSCs was also observed *in vivo* as HSCs purified from old irradiated mice failed to induce γH2AX foci (Fig. 6d, e). These data indicate that ATM signalling in response to acute DNA damage induction is compromised in old HSCs. This deficit in ATM signalling did not however impact the ability of old HSCs to repair DSBs as young and old HSCs exhibited similar kinetics of repair as indicated by time-course resolution of comet tails and 53BP1 foci post-irradiation (Fig. 6f, g). To explore if the reduced ATM activity of old HSCs could be linked to diminished apoptotic priming, we analysed apoptotic priming in LSKs and MPs from young and old mice in response to IR in the presence or absence of the ATM inhibitor KU-55933[52] at a dose that inhibited ATM-dependent γH2AX activity in LSK and c-kit enriched cells (Supplementary Figure 6d, e). ATM inhibition was sufficient to significantly reduce apoptotic priming in both young and old LSKs and MPs upon exposure to IR (Fig. 6h) and to increase the survival of young irradiated HSCs (Fig. 6i). These results suggest that ATM plays a role in regulating apoptotic priming in haematopoietic progenitor cells, and raise the possibility that the diminished apoptotic priming associated with HSC ageing may be underwritten by diminished ATM signalling. As apoptotic priming was elevated upon transplantation of old

HSCs into young irradiated recipients (Fig. 4a, b), we tested whether ATM signalling (Fig. 6a-c) was concomitantly restored post-transplantation into young hosts. To address this we analysed the marrow of mice that had been transplanted 21-23 weeks previously with young or old whole bone marrow (Supplementary Figure 4a). Strikingly, untreated young and old HSCs analysed post-transplantation showed comparable basal levels of γH2AX and 53BP1 (Fig. 6j, k) and a comparable ability to induce γH2AX and 53BP1 foci upon irradiation irrespective of donor age (Fig. 6j, k) indicating that ATM activity had been restored in old HSCs upon transplantation into a young host.

Discussion

In this study, we show that old HSCs are more resistant to DNA damage induced apoptosis than young HSCs regardless of the type of DNA lesion induced. This generalized response points towards a common mechanism underlying the survival advantage of old HSCs rather than differential activity of specific DNA repair pathways. Indeed, using BH3 profiling we show that during ageing HSCs become less primed for apoptosis underwritten by diminution of BIM/BAX, BID/BAK and BAD/BCL-2 responses. We discovered that the survival advantage of old HSCs in response to DNA damage induction could be reset to a level comparable with young HSCs upon transplantation into young hosts suggesting an important role for the microenvironment in regulating apoptotic priming. In addition, we uncovered a role for ATM in regulating apoptotic priming and survival in haematopoietic progenitors and showed that old HSCs have diminished ATM activity in response to acute DNA damage induction. Whether ageing associated cellular alterations in the niche, differences in downstream blood progenitor/effectors, or humoral signals emanating from the microenvironment underlie the differential regulation of apoptosis of HSCs during ageing impinge directly on ATM activity or represent independent mechanisms is still unclear. Nonetheless, the fact that transplantation into a young host restored ATM activity in old HSCs concomitant with normalization of apoptotic priming and survival of HSCs in response to DNA damage induction suggests that the aged niche may play a critical role in regulating ATM activity and the DNA damage response during HSC ageing. Taken together, these results suggest that the diminished apoptotic priming observed in old HSCs could underlie the perpetuation of the stem cell pool even in the face of DNA damage by providing a selective advantage to old HSCs that are rendered insensitive to DNA lesions that would otherwise kill their younger counterparts. Consistent with this idea, p53 has been shown to act as a critical mediator of cell competition in stem and progenitor cells with levels of DNA damage that do not reach a threshold high enough to activate apoptosis allowing damaged stem cells to survive and propogate[53]. In a comparable manner, diminution of apoptotic priming provides a mechanism allowing damaged HSCs, particularly myeloid-biased HSCs, to survive and propagate in the aged marrow thereby contributing to the oligoclonal expansion of the HSC compartment observed in mice and humans[14,37,39,54]. Such a selective advantage may also underlie the accrual of DNA damage in the HSC compartment[4,55–59] ultimately leading to ageing-associated hematopoietic malignancies.

Methods

Results presented in this study are drawn from each and every experiment that did not fail for technical reasons, and only experiments that failed for technical reasons were excluded. No other exclusion criteria were applied.

Mice

All mice used were C57BL/6 males. Young mice were 12-14 weeks old. Old mice were obtained from the National Institute on Aging and were 24–26 months old. All mice were maintained according to protocols approved by Harvard Medical School Animal Facility Administrative Panel on Laboratory Animal Care, and all procedures were performed with consent from the local ethics committees (IACUC Harvard Protocol 04428).

Purification of Cells

Adult bone marrow cells were extracted by crushing the bones of donor mice. Cells were enriched using c-kit magnetic beads (Miltenyi) and stained with the following cell-surface antibodies for 1.5 hours on ice:

Lin cocktail (Mac1, Gr1, Ter119, B220, CD3, CD4, CD8), c-kit, Sca-1, CD34, Flk2, FcγR, IL7Ra, CD150, CD45.1 and CD45.2. All cells were sorted on a FACSAria II (Becton Dickinson), and propidium iodide was used to exclude dead cells.

Cell Culture

Cells were clone sorted into 96-well round-bottom plates. HSCs were cultured in S-Clone (Iwai North America Inc.) supplemented with 0.75% AlbuMAX-I (Gibco), 1x penicillin/streptomycin, 50 mM 2-mercaptoethanol (Invitrogen) and the following cytokines: 20 ng/ml mouse stem cell factor, 20 ng/ml mouse thrombopoietin, 20 ng/ml mouse IL-12. Myeloid progenitors and c-kit enriched cells were cultured in Dulbecco's modified Eagle's medium and F-12 medium (Gibco and Invitrogen) supplemented with 10% fetal calf serum (Hyclone and Thermo Scientific), 1x penicillin/streptomycin, 2 mM GlutaMAX, 50 mM 2-mercaptoethanol (Invitrogen), and the following cytokines: 20 ng/ml mouse stem cell factor, 20 ng/ml mouse thrombopoietin, 20 ng/ml mouse IL-3, 20 ng/ml mouse granulocyte macrophage colony-stimulating factor (all purchased from PeproTech). c-kit enriched bone marrow (2×10^6 cells/ml) were exposed for 4 hours to 10 μM ATMi (KU55933, Selleckchem). All cells were kept in a 5% O_2 incubator.

Survival assays

For each experiment, 24-48 individual cells from individual mice were analysed. Cells were either irradiated with 2Gy or treated for 18 hours with 0.2 mg/ml ethyl-nitrosourea, 0.2 mg/ml ethyl-methanesulfonate, 0.5mM hydroxyurea, or 250ng/ml Doxorubicin (all from Sigma). For HSC survival upon ATM inhibition, single cells were pre-treated with 10 μM ATMi (KU55933, Selleckchem) for 4 hours and the irradiated with 2Gy. After the incubation time, media was refreshed with drug-free media. Cells were incubated at 37° C in a humidified atmosphere with 5% CO_2. At 8 days of culture, colonies were counted under the microscope. At 10 days of culture, the size of each colony was measured under a

microscope. For the cell growth dynamics assay, either freshly isolated young and old or donor-derived young and old HSCs were counted under the microscope every 24 hours for 8 days. Viability was determined by appearance.

AnnexinV assays

HSCs and MPs were isolated and either stained immediately after purification or irradiated and kept in culture for 8 hours. Cells were stained following the manufacturer's protocol (Annexin V Apoptosis Detection kit, BD Pharmingen).

Transplantation

For competitive transplantation upon DNA damage induction, 500 CD45.2 HSCs or CD150 high, low or negative HSCs were transplanted into lethally irradiated (10 Gy) CD45.1 8-12-week-old female recipients along with 3×10^5 competitor congenic bone marrow cells. For non-competitive transplantation, 5 million whole bone marrow cells were transplanted into lethally irradiated (10 Gy) CD45.1 8-12-week-old female recipients or 17 month old CD45.2 males. Peripheral blood analysis was performed at 4-week intervals post-transplantation using antibodies against Ter119, B220, Mac1, Gr1, CD3, CD45.1, CD45.2. Propidium iodide was used to exclude dead cells.

BH3 profiling

Bone marrow cells from young and old mice or from transplanted mice were isolated, c-kit enriched using separation columns (Miltneyi) and stained with antibodies to identify bone marrow populations as described above. For BH3 profiling, cells were resuspended at 2×10^6 cells/mL and incubated with 20 μg/ml oligomycin, 0.0005% digitonin and BH3 peptides at indicated concentrations (amino acid peptide sequences for BH3 peptides[60]) in DTEB buffer (135 mM Trehalose, 10 mM HEPES-KOH, 0.1% w/v BSA, 20 μM EDTA, 20 μM EGTA, 50 mM KCl, 5 mM succinate, final pH 7.4) for 30 minutes (BIM and BID) or 60 minutes (BAD, HRK and NOXA). Fifteen minutes prior to the completion of the peptide incubation, Tetramethylrhodamine (TMRE) was added to a final concentration of 20 nM. Cells were analysed by flow cytometry to assess mitochondrial depolarization on BD Canto II Analyzer. Peptide and TMRE incubation was performed on heating blocks at 22°C. The % depolarization, was calculated from the median fluorescence intensity (MFI)) of the TMRE peak as:

$$\%\ \text{Depolarization/Priming} = 100 \times (1 - ([\text{MFI}_{\text{Peptide}} - \text{MFI}_{\text{FCCP}}] \div [\text{MFI}_{\text{DMSO}} - \text{MDI}_{\text{FCCP}}]))$$

Analysis was done using FlowJo and GraphPad Prism.

Immunostaining

HSCs were sorted, irradiated and kept in culture for 1 hour in SClone media and then fixed with 4% paraformaldehyde for 30 minutes at RT. Cells were permeabilized (0.1% Triton, 2% goat serum in PBS) for 15 minutes at RT, blocked (2% goat serum with 0.03% Tween in PBS) for 1 hour at RT and incubated with primary antibodies anti-γH2AX (BioLegend) and anti-53BP1 (Novus Biologicals) at 1:1000 dilution for 36 hours at 4° C. Then, HSCs were

incubated with secondary antibodies anti-rabbit Alexa Flour 594 (A21207) and anti-mouse Alexa Flour488 (A10667) for 1 hour at RT. To visualize the nuclei the cells were counterstained by DAPI. In order to remove the permeabilization solution, primary and secondary antibodies respectively, the cells were several times washed in 0.03% Tween in PBS. Finally, the cells were transferred to slides and mounted on Vecta-Mount. Images were acquired on Carl Zeiss Observer Z.1 fluourescent microscope and processed by ImageJ 1.49v. Several hundreds of HSCs from 4 (53BP1) and 6 (γH2AX) experiments were scored blindly. Foci were counted manually and statistic was done using GraphPad Prism.

Dot Blot

LSKs were sorted, irradiated and cultured in F12 complete media for 1 hour. Then, cells were lysed in modified Laemmli buffer (240 mM Tris/HCl pH 6.8, 8% SDS, 5% beta-mercaptoethanol) at 5×10^5 cells/ml and incubated 10 minutes at 99° C. 30×10^5 LKSs were spotted on a 0.2μm nitrocellulose membrane (BioRad), let dry, washed with PBST (0.1% Tween20 in PBS) and blocked overnight at 4° C in 5% BSA in PBST. Primary antibodies (anti -H2A.X Phospho Ser139 from BioLegend and actin from Santa-Cruz) were used at 1/1000 for 2 hours RT in 0.5% BSA in PBST. Secondary antibodies (anti-mouse HRP, Santa Cruz and anti-goat HRP, Jackson) were incubated at 1/2000 in 0.5% BSA in PBST. Membranes were washed 3 times for 15 minutes in PBST. Dot blot was developed using SuperSignal West Femto (ThermoFisher Scientific) and Amersham Hyperfilm ECL (GE Healthcare).

Comet assay

Young and old HSCs were sorted, irradiated (2Gy) and cultured in S-Clone for 1h. Then, alkaline comet assays were done as described previously[4].

Statistics and Reproducibility

Statistical analysis (Two-tailed Student’s t-test and LogRank test) was performed using GraphPad Prism. Experiments were repeated at least three times, except those in Figures 2a, 2c, 3d, 5e, S2d, S2e, S2f, S2g and S3e, which were repeated twice and Figures 2b, 2d, 4e, 4f, 4g, 6d, 6e, 6f, 6g, 6i, S5a, S5b, S5d, S5e, S6c and S6e, which were performed once. Experiments that were only performed once or twice include multiple biological replicates (survival, transplants, BH3 profiling after ATMi) or are assays in which different experiments should not be pooled and compared (comet assay). When data were pooled from different experiments, all replicates were done in the same conditions.

Data availability

Source data have been provided as Supplementary Table 1. All other data supporting the findings of this study are available from the corresponding author on reasonable request.

Supplementary Material

Refer to Web version on PubMed Central for supplementary material.

Acknowledgments

We would like to thank J.A. Garcia-Martin for developing the script used to generate Supplementary Figure 3, E. Shlevkov for help with statistics, U. Rajarajacholan for help with dot blots and all the members of the D.J.R. laboratory for help. The A.N. laboratory was supported by the Intramural Research Program of the NIH, the National Cancer Institute, the Center for Cancer Research, and the Alex Lemonade Stand Foundation Award. L.H was supported by NIH fellowship F31CA186301. The A.L. laboratory was supported by NIH grant P01 CA066996 and Leukemia and Lymphoma Society Grant TRP6387-13. D.J.R. is supported by grants from the NIH (RO1HL107630, R00AG029760, and UO1DK072473-01) as well as grants from The Leona M. and Harry B. Helmsley Charitable Trust, The New York Stem Cell Foundation, The Harvard Stem Cell Institute, and American Federation for Aging Research.

References

1. Rossi DJ, Jamieson CH, Weissman IL. Stems cells and the pathways to aging and cancer. Cell. 2008; 132:681–696. [PubMed: 18295583]
2. Geiger H, de Haan G, Florian MC. The ageing haematopoietic stem cell compartment. Nat Rev Immunol. 2013; 13:376–389. [PubMed: 23584423]
3. Beerman I, Maloney WJ, Weissmann IL, Rossi DJ. Stem cells and the aging hematopoietic system. Curr Opin Immunol. 2010; 22:500–506. [PubMed: 20650622]
4. Beerman I, Seita J, Inlay MA, Weissman IL, Rossi DJ. Quiescent Hematopoietic Stem Cells Accumulate DNA Damage during Aging that Is Repaired upon Entry into Cell Cycle. Cell Stem Cell. 2014
5. Rossi DJ, et al. Deficiencies in DNA damage repair limit the function of haematopoietic stem cells with age. Nature. 2007; 447:725–729. [PubMed: 17554309]
6. Nijnik A, et al. DNA repair is limiting for haematopoietic stem cells during ageing. Nature. 2007; 447:686–690. [PubMed: 17554302]
7. Walter D, et al. Exit from dormancy provokes DNA-damage-induced attrition in haematopoietic stem cells. Nature. 2015; 520:549–552. [PubMed: 25707806]
8. Rube CE, et al. Accumulation of DNA damage in hematopoietic stem and progenitor cells during human aging. PLoS ONE. 2011; 6:e17487. [PubMed: 21408175]
9. Rossi DJ, et al. Cell intrinsic alterations underlie hematopoietic stem cell aging. Proc Natl Acad Sci U S A. 2005; 102:9194–9199. [PubMed: 15967997]
10. Chambers SM, et al. Aging hematopoietic stem cells decline in function and exhibit epigenetic dysregulation. PLoS Biol. 2007; 5:e201. [PubMed: 17676974]
11. Beerman I, et al. Proliferation-dependent alterations of the DNA methylation landscape underlie hematopoietic stem cell aging. Cell Stem Cell. 2013; 12:413–425. [PubMed: 23415915]
12. Sun D, et al. Epigenomic profiling of young and aged HSCs reveals concerted changes during aging that reinforce self-renewal. Cell Stem Cell. 2014; 14:673–688. [PubMed: 24792119]
13. Florian MC, et al. Cdc42 activity regulates hematopoietic stem cell aging and rejuvenation. Cell Stem Cell. 2012; 10:520–530. [PubMed: 22560076]
14. Beerman I, et al. Functionally distinct hematopoietic stem cells modulate hematopoietic lineage potential during aging by a mechanism of clonal expansion. Proc Natl Acad Sci U S A. 2010; 107:5465–5470. [PubMed: 20304793]
15. Kim M, Moon HB, Spangrude GJ. Major age-related changes of mouse hematopoietic stem/progenitor cells. Ann N Y Acad Sci. 2003; 996:195–208. [PubMed: 12799297]
16. Morrison SJ, Wandycz AM, Akashi K, Globerson A, Weissman IL. The aging of hematopoietic stem cells. Nat Med. 1996; 2:1011–1016. [PubMed: 8782459]
17. Sudo K, Ema H, Morita Y, Nakauchi H. Age-associated characteristics of murine hematopoietic stem cells. J Exp Med. 2000; 192:1273–1280. [PubMed: 11067876]
18. BaguleyBC, , KerrDJ. Anticancer Drug DevelopmentAcademic Press; 2002
19. Brunelle JK, Letai A. Control of mitochondrial apoptosis by the Bcl-2 family. J Cell Sci. 2009; 122:437–441. [PubMed: 19193868]

20. Cory S, Adams JM. The Bcl2 family: regulators of the cellular life-or-death switch. Nat Rev Cancer. 2002; 2:647–656. [PubMed: 12209154]
21. Llambi F, et al. A unified model of mammalian BCL-2 protein family interactions at the mitochondria. Mol Cell. 2011; 44:517–531. [PubMed: 22036586]
22. Letai A, et al. Distinct BH3 domains either sensitize or activate mitochondrial apoptosis, serving as prototype cancer therapeutics. Cancer Cell. 2002; 2:183–192. [PubMed: 12242151]
23. Ren D, et al. BID, BIM, and PUMA are essential for activation of the BAX- and BAK-dependent cell death program. Science. 2010; 330:1390–1393. [PubMed: 21127253]
24. Hockenbery D, Nunez G, Milliman C, Schreiber RD, Korsmeyer SJ. Bcl-2 is an inner mitochondrial membrane protein that blocks programmed cell death. Nature. 1990; 348:334–336. [PubMed: 2250705]
25. Oda E, et al. Noxa, a BH3-only member of the Bcl-2 family and candidate mediator of p53-induced apoptosis. Science. 2000; 288:1053–1058. [PubMed: 10807576]
26. Boyd JM, et al. Bik, a novel death-inducing protein shares a distinct sequence motif with Bcl-2 family proteins and interacts with viral and cellular survival-promoting proteins. Oncogene. 1995; 11:1921–1928. [PubMed: 7478623]
27. Kutuk O, Letai A. Regulation of Bcl-2 family proteins by posttranslational modifications. Curr Mol Med. 2008; 8:102–118. [PubMed: 18336291]
28. Del Gaizo Moore V, Letai A. BH3 profiling–measuring integrated function of the mitochondrial apoptotic pathway to predict cell fate decisions. Cancer Lett. 2013; 332:202–205. [PubMed: 22230093]
29. Ni Chonghaile T, et al. Pretreatment mitochondrial priming correlates with clinical response to cytotoxic chemotherapy. Science. 2011; 334:1129–1133. [PubMed: 22033517]
30. Ryan JA, Brunelle JK, Letai A. Heightened mitochondrial priming is the basis for apoptotic hypersensitivity of CD4+ CD8+ thymocytes. Proc Natl Acad Sci U S A. 2010; 107:12895–12900. [PubMed: 20615979]
31. Vo TT, et al. Relative mitochondrial priming of myeloblasts and normal HSCs determines chemotherapeutic success in AML. Cell. 2012; 151:344–355. [PubMed: 23063124]
32. Sarosiek KA, et al. Developmental Regulation of Mitochondrial Apoptosis by c-Myc Governs Age- and Tissue-Specific Sensitivity to Cancer Therapeutics. Cancer Cell. 2017; 31:142–156. [PubMed: 28017613]
33. Sarosiek KA, et al. BID preferentially activates BAK while BIM preferentially activates BAX, affecting chemotherapy response. Mol Cell. 2013; 51:751–765. [PubMed: 24074954]
34. Opferman JT, et al. Obligate role of anti-apoptotic MCL-1 in the survival of hematopoietic stem cells. Science. 2005; 307:1101–1104. [PubMed: 15718471]
35. Campbell CJ, et al. The human stem cell hierarchy is defined by a functional dependence on Mcl-1 for self-renewal capacity. Blood. 2010; 116:1433–1442. [PubMed: 20525924]
36. Villunger A, et al. p53- and drug-induced apoptotic responses mediated by BH3-only proteins puma and noxa. Science. 2003; 302:1036–1038. [PubMed: 14500851]
37. Dykstra B, Olthof S, Schreuder J, Ritsema M, de Haan G. Clonal analysis reveals multiple functional defects of aged murine hematopoietic stem cells. J Exp Med. 2011; 208:2691–2703. [PubMed: 22110168]
38. Muller-Sieburg CE, Cho RH, Karlsson L, Huang JF, Sieburg HB. Myeloid-biased hematopoietic stem cells have extensive self-renewal capacity but generate diminished lymphoid progeny with impaired IL-7 responsiveness. Blood. 2004; 103:4111–4118. [PubMed: 14976059]
39. Benz C, et al. Hematopoietic stem cell subtypes expand differentially during development and display distinct lymphopoietic programs. Cell Stem Cell. 2012; 10:273–283. [PubMed: 22385655]
40. Challen GA, Boles NC, Chambers SM, Goodell MA. Distinct hematopoietic stem cell subtypes are differentially regulated by TGF-beta1. Cell Stem Cell. 2010; 6:265–278. [PubMed: 20207229]
41. Morita Y, Ema H, Nakauchi H. Heterogeneity and hierarchy within the most primitive hematopoietic stem cell compartment. J Exp Med. 2010; 207:1173–1182. [PubMed: 20421392]
42. Beerman I, Rossi DJ. Epigenetic Control of Stem Cell Potential during Homeostasis, Aging, and Disease. Cell Stem Cell. 2015; 16:613–625. [PubMed: 26046761]

43. Seita J, et al. Gene Expression Commons: an open platform for absolute gene expression profiling. PLoS ONE. 2012; 7:e40321. [PubMed: 22815738]
44. Lukas C, et al. Mdc1 couples DNA double-strand break recognition by Nbs1 with its H2AX-dependent chromatin retention. Embo J. 2004; 23:2674–2683. [PubMed: 15201865]
45. Bakkenist CJ, Kastan MB. DNA damage activates ATM through intermolecular autophosphorylation and dimer dissociation. Nature. 2003; 421:499–506. [PubMed: 12556884]
46. D'Amours D, Jackson SP. The Mre11 complex: at the crossroads of dna repair and checkpoint signalling. Nat Rev Mol Cell Biol. 2002; 3:317–327. [PubMed: 11988766]
47. Ito K, et al. Regulation of oxidative stress by ATM is required for self-renewal of haematopoietic stem cells. Nature. 2004; 431:997–1002. [PubMed: 15496926]
48. Maryanovich M, et al. The ATM-BID pathway regulates quiescence and survival of haematopoietic stem cells. Nat Cell Biol. 2012; 14:535–541. [PubMed: 22446738]
49. Burma S, Chen BP, Murphy M, Kurimasa A, Chen DJ. ATM phosphorylates histone H2AX in response to DNA double-strand breaks. J Biol Chem. 2001; 276:42462–42467. [PubMed: 11571274]
50. Flach J, et al. Replication stress is a potent driver of functional decline in ageing haematopoietic stem cells. Nature. 2014; 512:198–202. [PubMed: 25079315]
51. Schultz LB, Chehab NH, Malikzay A, Halazonetis TD. p53 binding protein 1 (53BP1) is an early participant in the cellular response to DNA double-strand breaks. J Cell Biol. 2000; 151:1381–1390. [PubMed: 11134068]
52. Hickson I, et al. Identification and characterization of a novel and specific inhibitor of the ataxia-telangiectasia mutated kinase ATM. Cancer Res. 2004; 64:9152–9159. [PubMed: 15604286]
53. Bondar T, Medzhitov R. p53-mediated hematopoietic stem and progenitor cell competition. Cell Stem Cell. 2010; 6:309–322. [PubMed: 20362536]
54. Pang WW, et al. Human bone marrow hematopoietic stem cells are increased in frequency and myeloid-biased with age. Proc Natl Acad Sci U S A. 2011; 108:20012–20017. [PubMed: 22123971]
55. Jan M, et al. Clonal evolution of preleukemic hematopoietic stem cells precedes human acute myeloid leukemia. Sci Transl Med. 2012; 4:149ra118.
56. Ley TJ, et al. DNMT3A mutations in acute myeloid leukemia. N Engl J Med. 2010; 363:2424–2433. [PubMed: 21067377]
57. Jaiswal S, et al. Age-related clonal hematopoiesis associated with adverse outcomes. N Engl J Med. 2014; 371:2488–2498. [PubMed: 25426837]
58. Busque L, et al. Recurrent somatic TET2 mutations in normal elderly individuals with clonal hematopoiesis. Nat Genet. 2012; 44:1179–1181. [PubMed: 23001125]
59. Xie M, et al. Age-related mutations associated with clonal hematopoietic expansion and malignancies. Nat Med. 2014; 20:1472–1478. [PubMed: 25326804]
60. Ryan J, Letai A. BH3 Profiling in Whole Cells by Flourimeter or FACS. Methods. 2013

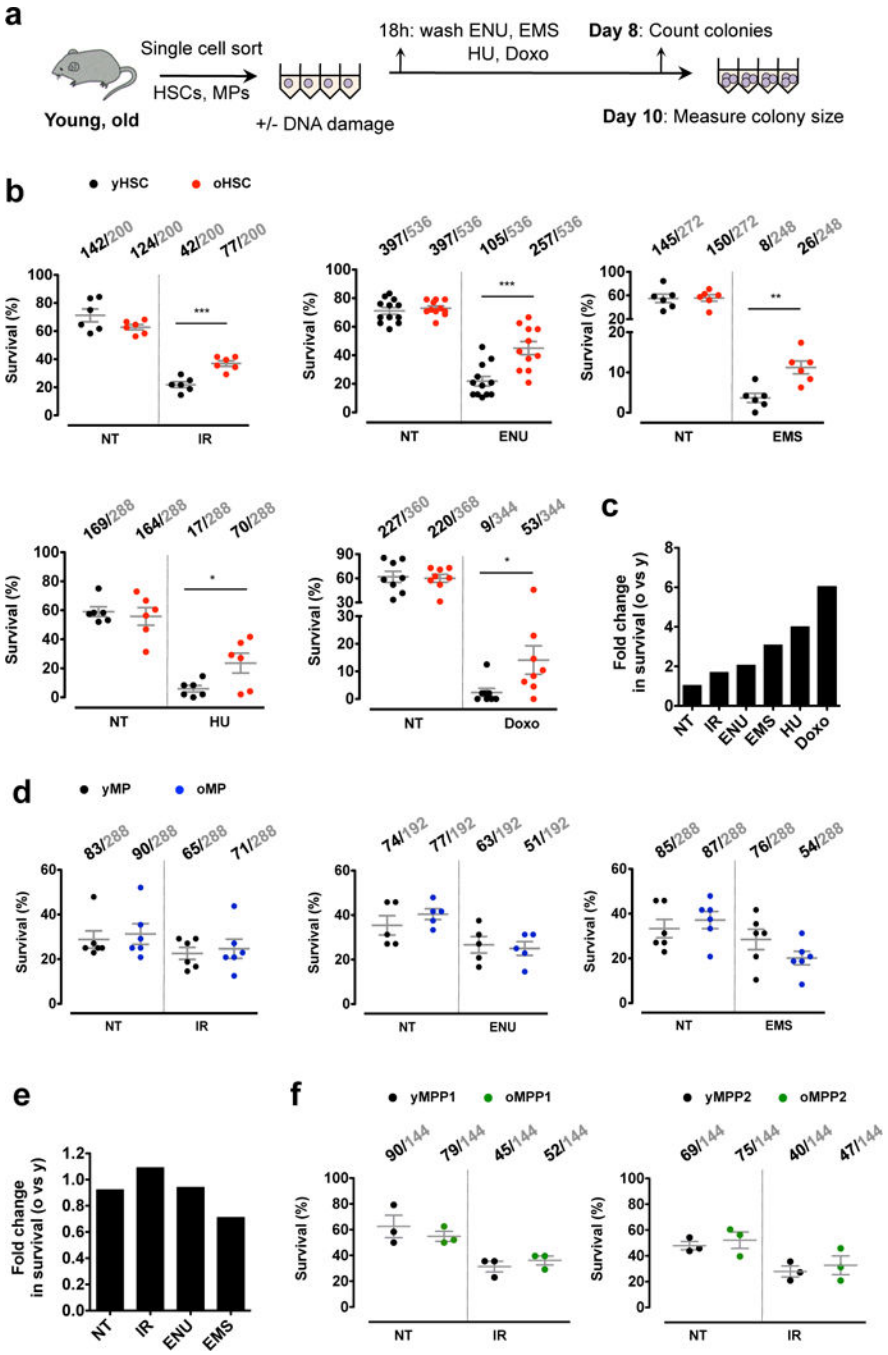

Figure 1. Old HSCs have increased survival upon DNA damage induction by a broad array of genotoxic agents

a) Schematic representation of experimental design. **b-c)** Colony forming potential of young and old HSCs showing **b)** clonal survival measured as a percentage of viable clones of non-treated (NT) versus treatment with the indicated genotoxic agent, and **c)** fold change in survival of old compared to young HSCs. Gamma irradiation (IR), ethyl-nitrosourea (ENU), ethyl-methanesulfonate (EMS), doxorrubicin (Doxo), hydroxyurea (HU). IR: data pooled from 5 independent experiments; ENU and Doxo: data pooled from 6 independent

experiments; EMS and HU: data pooled from 4 independent experiments. **d-e)** Colony forming potential of young and old myeloid progenitors (MPs) showing **d)** clonal survival measured as a percentage of viable clones in response to the indicated genotoxic agent, and **e)** fold change in survival of old compared to young MPs. IR: data pooled from 6 independent experiments; ENU: data pooled from 3 independent experiments; EMS: data pooled from 5 independent experiments. **f)** Clonal survival of young and old multipotent progenitors 1 and 2 (MPP1s, MPP2s) measured as a percentage of viable clones in response to IR. Data pooled from 3 independent experiments. For **b) d)** and **f)** each dot represents percent survival of cells from individual mice (n=3-12 mice). Numbers above the graphs indicate total number of surviving clones (black) vs total number of clones analysed (grey). $P<0.05$ (*), $P<0.005$ (**), $P<0.0005$ (***) (Two-tailed Student's t-test), centre bar represents mean and error bars represent SEM.

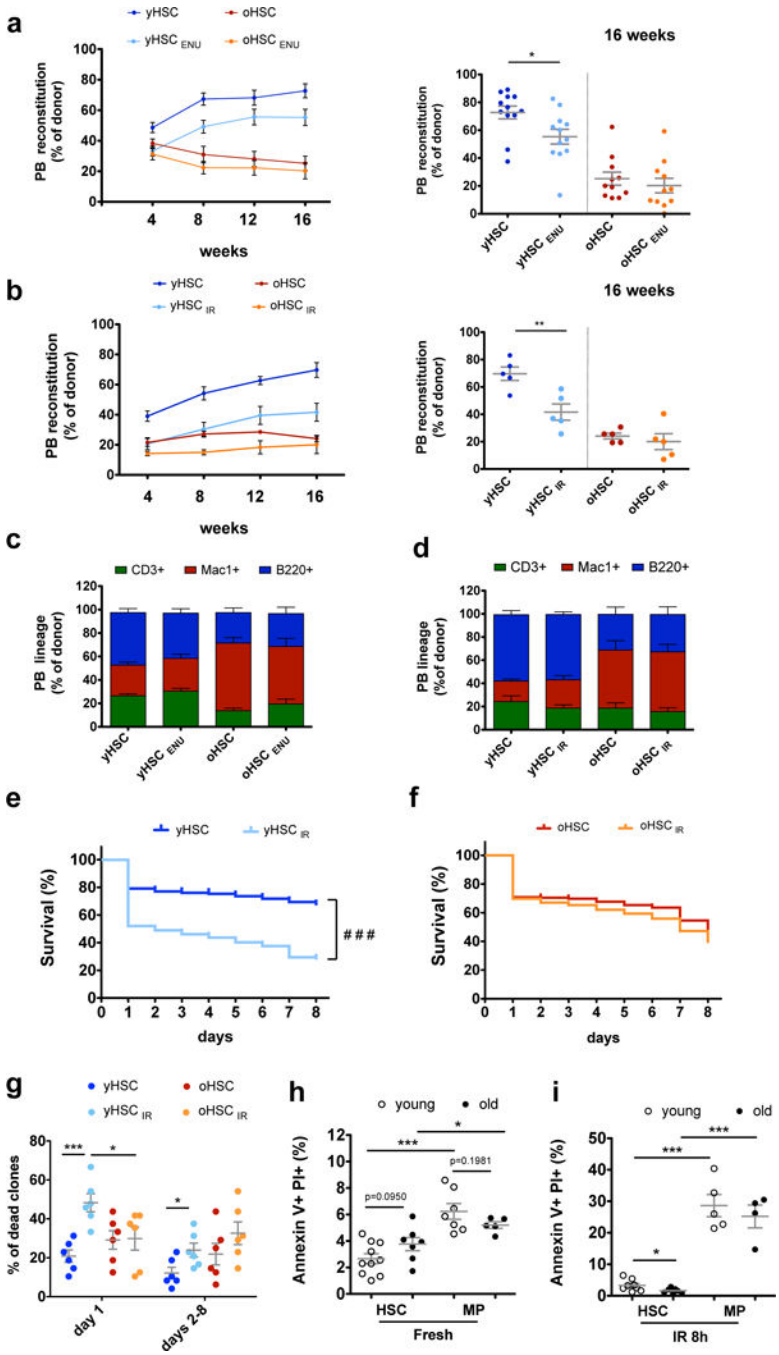

Figure 2. The function and viability of young and old HSCs is differentially impacted by DNA damage induction

a, c) Competitive transplantation of 500 young or old HSCs untreated or exposed to ENU (0.2 mg/ml for 18 hours) showing **a)** peripheral blood chimerism of recipient mice over the time course of the experiment, and individual recipients 16-weeks post-transplant, and **c)** lineage contribution of donor cells in recipients shown at week 16. **b, d)** Competitive transplantation of 500 young or old HSCs untreated or irradiated (2Gy) showing **b)** peripheral blood chimerism of recipient mice over the time course of the experiment, and

individual recipients 16-weeks post-transplant, and **d)** lineage contribution of donor cells in recipients shown at week 16. **e-f)** Kaplan-Mayer analysis showing survival measured daily for 8 days of **e)** untreated or irradiated (2Gy) young HSCs (yHSC, $yHSC_{IR}$), and **f)** untreated or irradiated (2Gy) old HSC (oHSC, $oHSC_{IR}$). **g)** Quantification of the number of clonal colonies that died either at day 1 or between days 2 through 8 post-plating. For **e-g)** 288 cells per condition were analysed, data pooled from n=6 independent experiments. **h, i)** Quantification of Annexin V+/PI+ in young and old HSCs and MPs in **h)** freshly isolated and **i)** 8 hour post irradiation with 2Gy (IR 8h). Data pooled from 4 independent experiments. Each dot represents cells from individual mice (n=5-10 mice). $P<0.05$ (*), $P<0.005$ (**), $P<0.0005$ (***) (Two-tailed Student's t-test), centre bar represents mean and error bars represent SEM. ###<0.0005 (LogRank test). Source data are included in Supplementary Table 1.

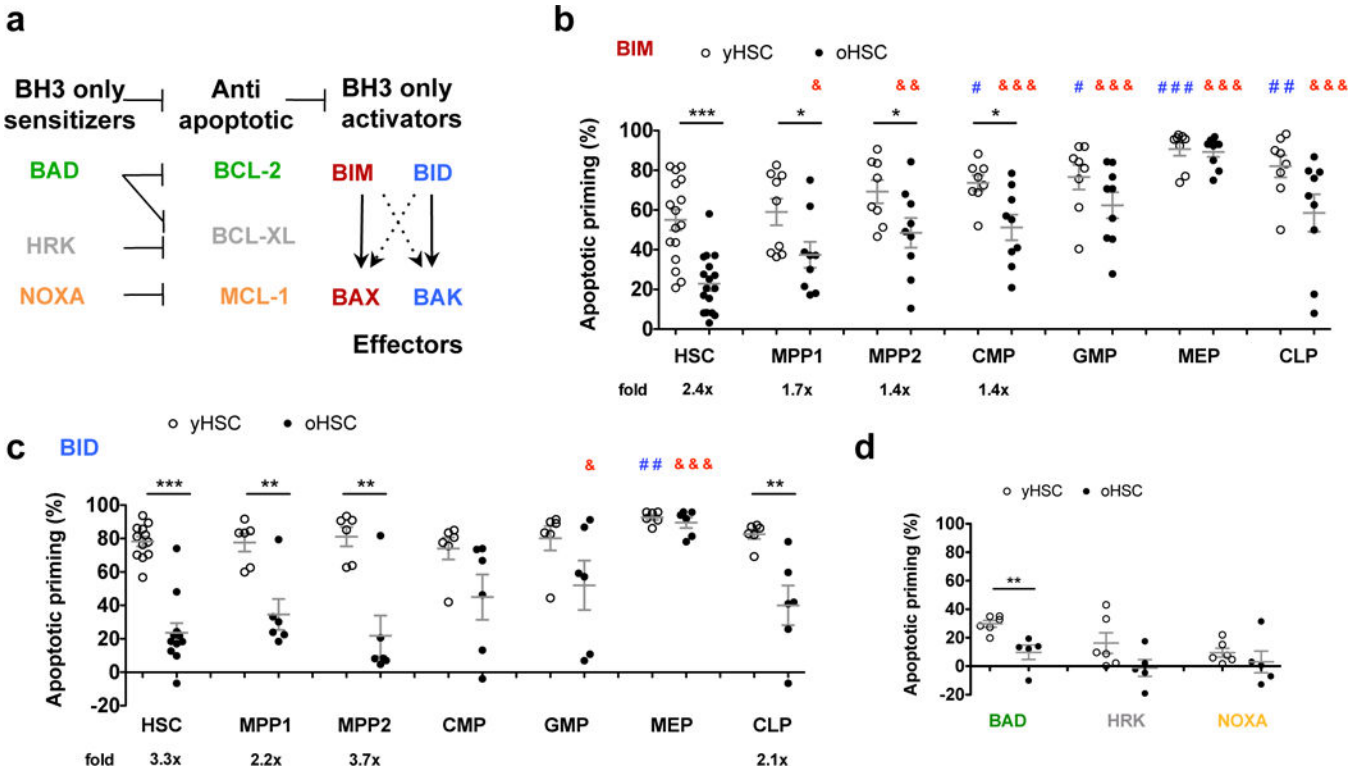

Figure 3. HSCs are the least apoptotically primed primitive progenitor population and exhibit differential dependence on apoptotic regulators during ageing

a) Schematic representation showing apoptotic pathway dependence of BH3 only sensitizers/activators and anti-apoptotic proteins. **b-c)** Apoptotic priming of the indicated haematopoietic stem and progenitors in young and old bone marrow in response to **b)** BIM (8 μM) and **c)** BID (8 μM). For **b)** data pooled from 8 independent experiments and for **c)** data pooled from 4 independent experiments, each dot represents cells from individual mice (n=8-16 mice). For **b)** and **c)**, comparisons made against HSCs are indicated as $^{\#, \#\#, \#\#\#}$ (blue, young) and $^{\&, \&\&, \&\&\&}$ (red, old). **d)** Apoptotic priming of young and old HSCs in response to BAD 80 μM, HRK 80 μM and NOXA 80 μM. each dot represents cells from individual mice (n=6 mice) Data pooled from 2 independent experiments. P< 0.05 **(*** $^{\# \&}$), P< 0.005 (** $^{\#\# \&\&}$), P< 0.0005 (*** $^{\#\#\# \&\&\&}$) (Two-tailed Student's t-test), centre bar represents mean and error bars represent SEM. Source data are included in Supplementary Table 1.

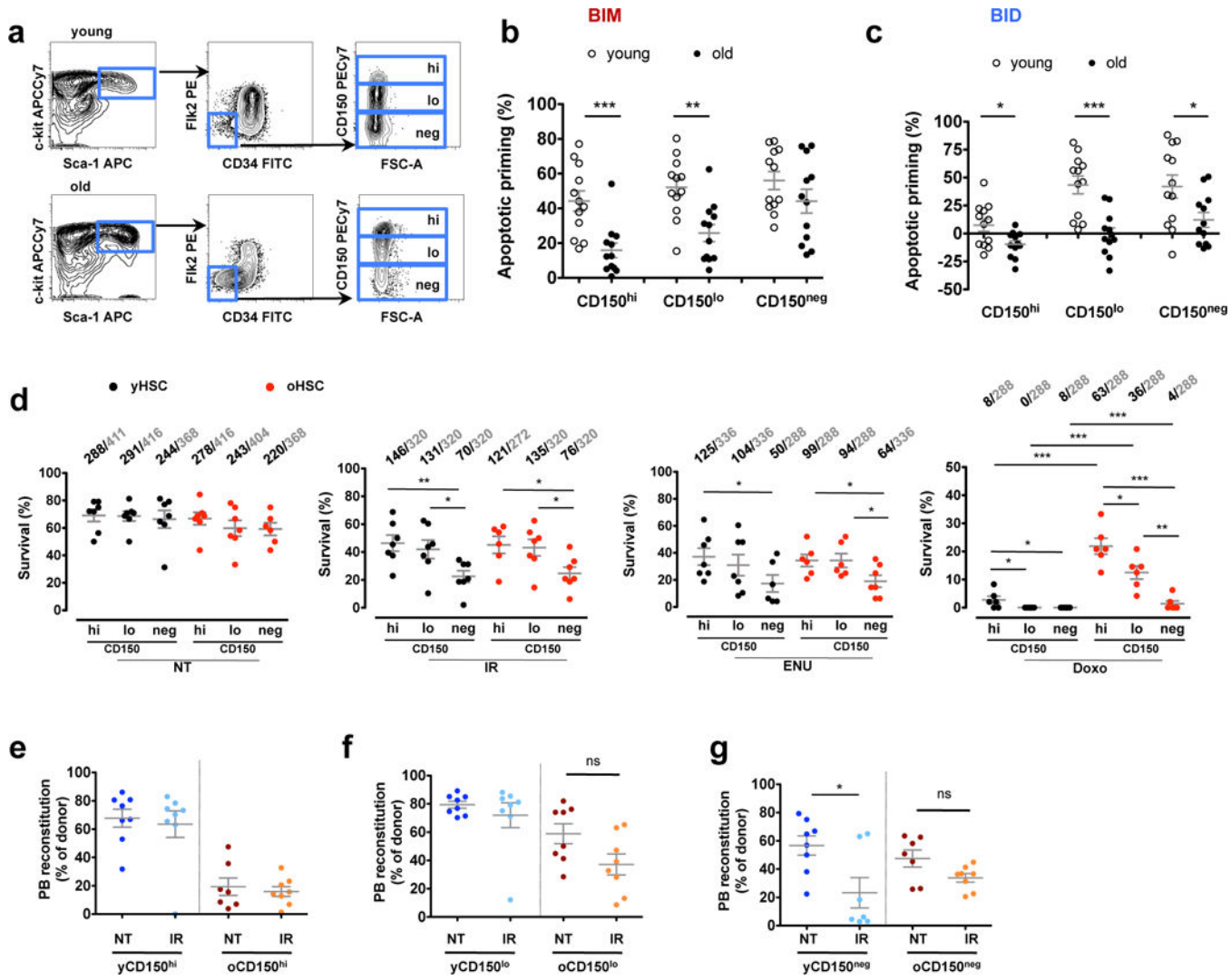

Figure 4. Apoptotic priming and survival upon DNA damage induction in HSC subsets

a) Representative gating strategy of young and old LSK, HSC and CD150 subsets. **b, c)** Apoptotic priming of young and old HSC subsets in response to **b)** BIM (8 μM) and **c)** BID (3 μM). Each dot represents cells from individual mice (n=12 mice). Data was pooled from 4 independent experiments. **d)** Clonal survival of young and old HSC subsets measured as a percentage of viable clones of non-treated (NT) versus treatment with the indicated genotoxic agent. Each dot represents percent survival of 24 to 48 single cells purified from individual mice. Numbers above the graphs indicate total number of surviving clones (black) vs total number of clones analysed (grey). IR and ENU: Data pooled from 7 independent experiments. Doxo: Data pooled from 5 independent experiments **e-g)** Competitive transplantation of 500 young and old **e)** CD150^{high}, **f)** CD150^{low} and **g)** CD150^{negative} HSCs subsets untreated or irradiated (2Gy) showing individual recipients 16-weeks post-transplant. Data represent 1 experiment, n=7-8 mice per group (each dot represents individual recipient mice). P< 0.05 **(***), P< 0.005 (**), P< 0.0005 (***) (Two-tailed Student's t-test), centre bar represents mean and error bars represent SEM. Source data are included in Supplementary Table 1.

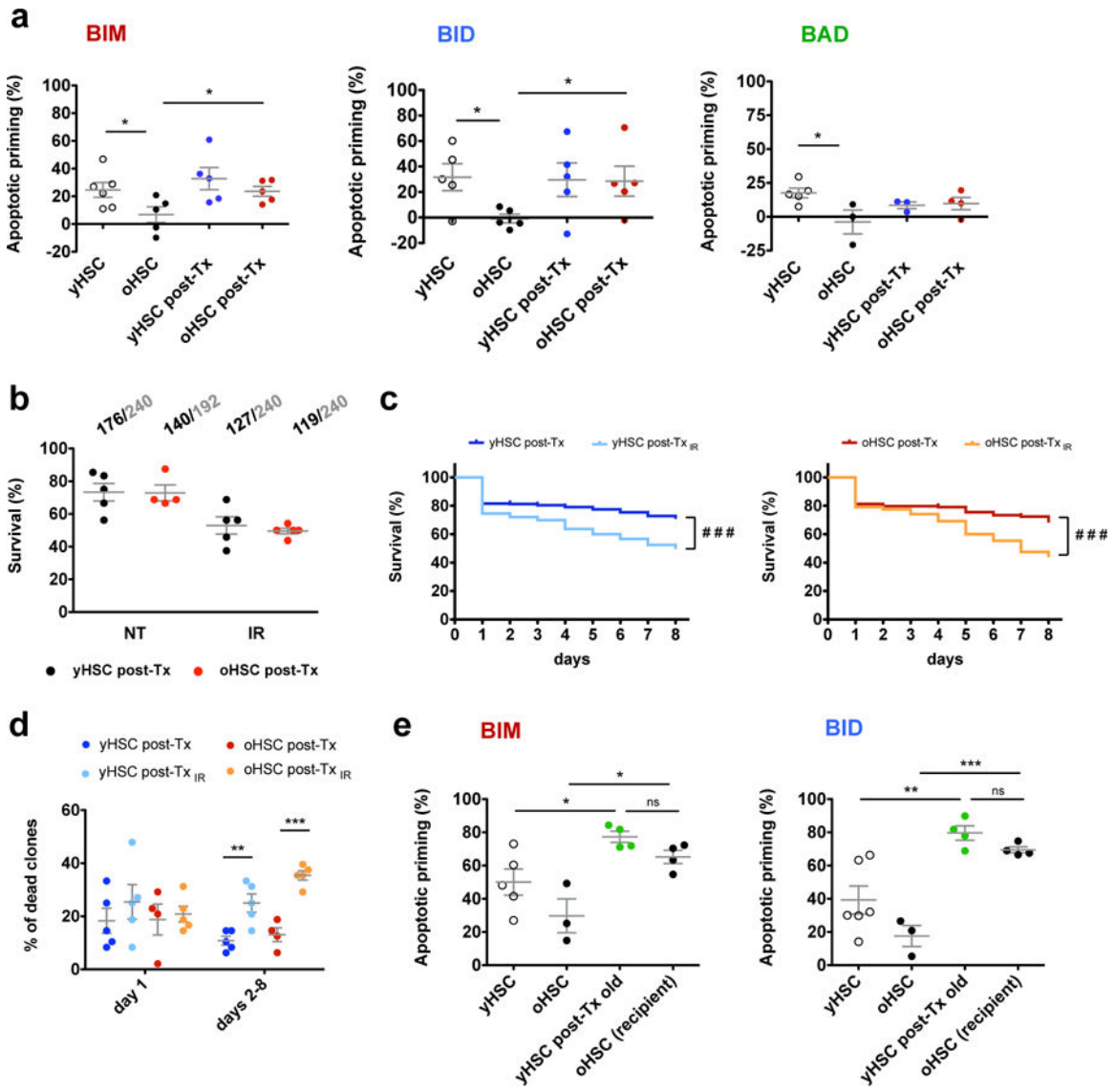

Figure 5. Apoptotic priming and survival upon DNA damage induction is equalized upon transplantation

a) Apoptotic priming of HSCs (LSK CD34-/lo CD150+) in response to BIM (8 μM), BID (3 μM) and BAD (80 μM) in steady-state young and old bone marrow and in bone marrow transplant-derived young and old LSK and MP (21-23 weeks post-transplantation), n=3-5 mice (each dot represents individual recipient mice). Data pooled from 5 independent experiments. **b)** Clonal survival of donor-derived young and old HSCs measured as a percentage of viable clones of non-treated (NT) versus IR (2Gy). Each dot represents percent survival of 48 single HSCs (LSK CD34−/lo Flk2− and LSK CD34−/lo CD150+) purified from individual mice (n=4-5 mice). Numbers above the graphs indicate total number of surviving clones (black) vs total number of clones analysed (grey). Data pooled from 3 independent experiments. **c)** Kaplan-Mayer analysis showing survival of donor-derived young and old HSCs (yHSC post-Tx, yHSC post-Tx $_{IR,}$ oHSC post-Tx, oHSC post-Tx $_{IR}$; HSC: LSK CD34−/lo Flk2− and LSK CD34−/lo CD150+) 21-23 weeks post-

transplantation measured daily for 8 days. **d)** Quantification of the number of clonal colonies that died either at day 1 or between days 2 through 8 post-plating. n=4 or n=5 mice per group (each dot represents the percentage of cells from individual recipient mice), 192-244 cells per condition were evaluated in 3 independent experiments. **e)** Apoptotic priming of HSCs (LSK CD34−/lo CD150+) in response to BIM (8 μM) or BID (3 μM) in steady-state young and old bone marrow and in bone marrow transplant-derived young HSCs (21-23 weeks post-transplantation), n=3-6 mice per group (each dot represents individual recipient mice). Data pooled from 2 independent experiments. P<0.05 (*), P<0.005 (**), P<0.0005 (***) (Two-tailed Student's t-test), centre bar represents mean and error bars represent SEM. ###<0.0005 (LogRank test). Source data are included in Supplementary Table 1.

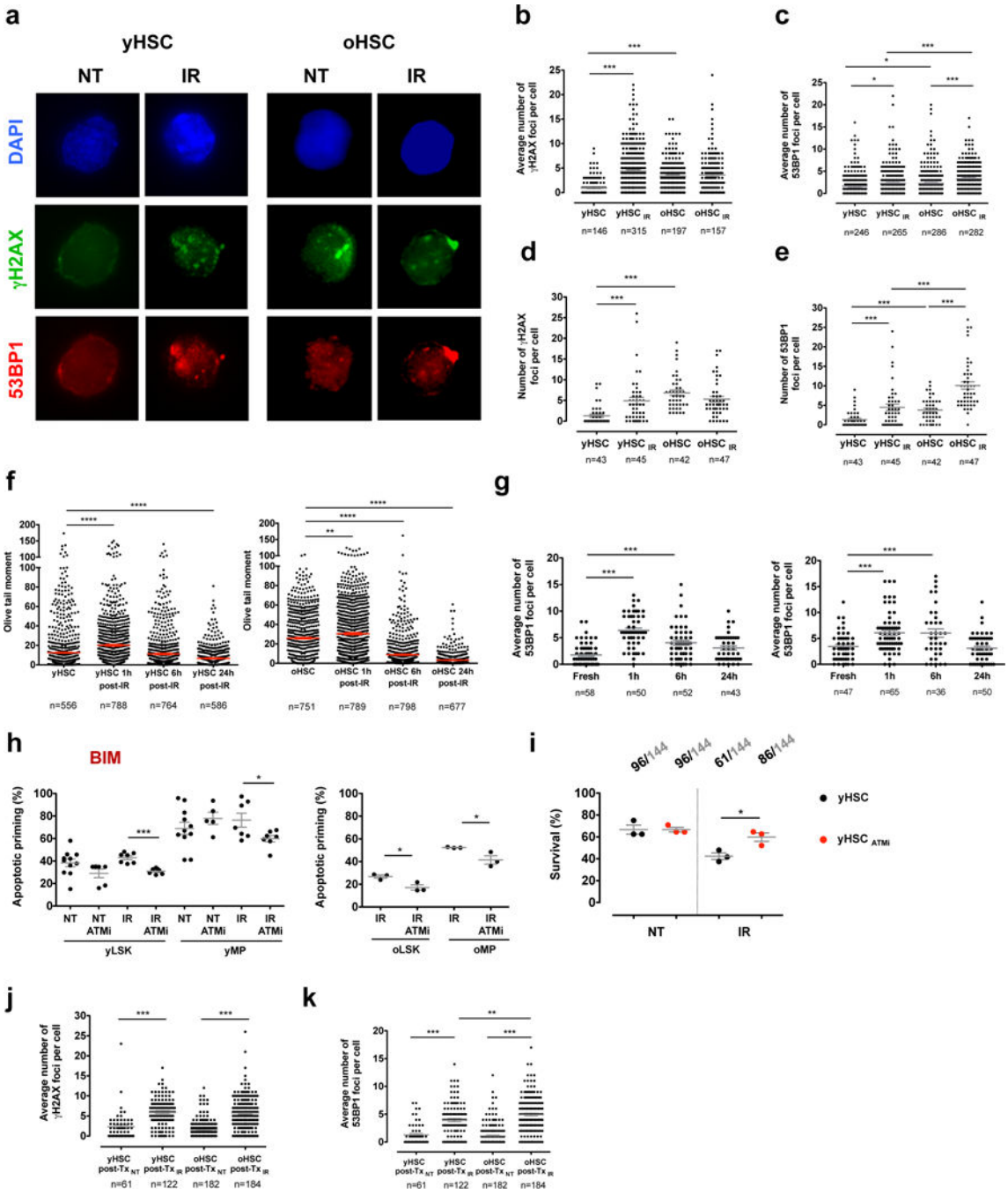

Figure 6. ATM activity is reduced in old HSCs and leads to a diminished apoptotoic priming response

a-c) Representative images and average number of **a-b)** γH2AX and **a-c)** 53BP1 foci in young and old HSCs upon 1 hour in culture with no treatment or irradiated (IR, 2Gy). Data pooled from 4 (γH2AX) and 6 (53BP1) independent experiments. **d-e)** Average number of **d)** γH2AX and **e)** 53BP1 foci in young and old HSCs upon 1 hour *in vivo* irradiation (IR, 10Gy). Data represent 1 experiment. **f)** Olive tail moment of young and old freshly isolated HSCs or upon 1, 6 and 24 hour in culture post irradiation with 2Gy. Data represent 1

experiment. **g)** 53BP1 foci of young and old freshly isolated HSCs or upon 1, 6 and 24 hour in culture post irradiation with 2Gy. Data represent 1 experiment. For **f)** and **g)** comparisons are made against freshly isolated young or old HSCs. **h)** Apoptotic priming of young and old LSK and MP upon 4h of culture with treatments in response to BIM 3μM IR (2Gy), ATMi (ATM inhibitor KU-55933, 10μM). n=3-12 mice per group (each dot represents individual mice). Data pooled from 5 individual experiments. **i)** Clonal survival of young HSCs measured as percentage of viable clones of non-treated (NT) versus IR (2Gy) upon 4h of ATMi pre-treatment. Each dot represents percent survival of 48 single HSCs purified from individual mice (n=3 mice). Numbers above the graphs indicate total number of surviving clones (black) vs total number of clones analysed (grey). Data represent 1 experiment. **j-k)** Average number of **j)** γH2AX and **k)** 53BP1 foci in young and old HSCs post 21-23 weeks of transplantation upon 1 hour in culture with no treatment or irradiated (IR, 2Gy). Data represent 1 experiment. For **b-g)** and **j)**, **k)** n numbers are stated below each panel and represent individual cells, indicated by dots. $P<0.05$ (*), $P<0.005$ (**), $P<0.0005$ (***) $P<0.0001$ (****), Two-tailed Student's t-test, centre bar represents mean and error bars represent SEM. Source data are included in Supplementary Table 1.